Earthquake Geotechnical Engineering for Protection and Development of Environment and Constructions – Silvestri & Moraci (Eds)
© 2019 Associazione Geotecnica Italiana, Rome, Italy, ISBN 978-0-367-14328-2

Liquefaction assessment of pumiceous sand with shear wave velocity approach

M.B. Asadi, R.P. Orense, M.S. Asadi & M.J. Pender
University of Auckland, Auckland, New Zealand

ABSTRACT: Natural pumiceous (NP) sands are a common volcanic soil found in the central part of the North Island, New Zealand. These NP sands have pumice components which are crushable and lightweight making them problematic in terms of engineering assessment of their geotechnical properties. Previous investigations on crushable volcanic soils indicate that penetration methods would not provide reliable estimates of their geotechnical properties. Thus, shear wave velocity (V_s) may be a promising alternative especially for estimating the cyclic resistance ratio (*CRR*) of crushable NP sands. In this paper, a number of cyclic triaxial and bender element tests are performed on three types of reconstituted NP sands to estimate their *CRR* and V_s, respectively. The results are then compared with those obtained from normal sands. The comparison indicates that using available *CRR*-V_s charts for normal sands would underestimate the *CRR* of NP sands since these materials have lower V_s and higher *CRR*.

1 INTRODUCTION

Ever since the phenomenon of liquefaction has been introduced to the geotechnical community, a significant number of liquefaction assessment studies using laboratory- and field-based approaches have been conducted on saturated sands (Youd et al., 2001). For example, Seed and Lee (1966) proposed a method for liquefaction assessment using the triaxial apparatus, while a simplified procedure introduced by Seed and Idriss (1971) utilized the standard penetration test (SPT) results for estimating the liquefaction resistance of soils. Later, additional field parameters, such as cone penetration test (CPT) tip resistance and shear wave velocity (V_s), were used to evaluate the cyclic resistance ratio (*CRR*) of soils (Youd et al., 2001).

While substantial investigations using field testing methodologies have been performed on granular soils which are considered to be hard-grained under normal loads, less is known about the applicability of such approaches in estimating the *CRR* of crushable volcanic soils, including natural pumiceous (NP) sands. These NP sands are a prominent soil type found in the central part of the North Island (NZ) and they are distributed over a large area due to the power of volcanic eruptions and, with subsequent airborne transport and later erosion and river transports, the pumice sands were mixed with other materials in the region. Pumice sands are characterized by distinctive features, such as compressibility, crushability, lightweight and vesicular nature (Orense et al., 2012). Figure 1 shows the complex surface texture of pumice particles with high angularity, enabling them to have a high angle of internal friction (Kikkawa et al., 2013).

In the last few decades, some studies have been performed to understand the applicability of penetration testing techniques for crushable volcanic soils. For example, CPT calibration chamber test results on pure pumice sands indicate that the cone penetration resistance is independent of the soil's relative density (D_r); however, the D_r of hard-grained soils significantly affects the cone resistance value (Wesley, 2006). In addition, Miura et al. (2003) reported that the manifestation of particle crushing during intrusion of SPT rod into some Japanese volcanic soil deposits considerably underestimated the stiffness of volcanic soils. Therefore, shear wave velocity (V_s) profiling, a non-destructive testing method, may be a promising alternative for assessing the liquefaction resistance of crushable NP sands in the field. Note however that

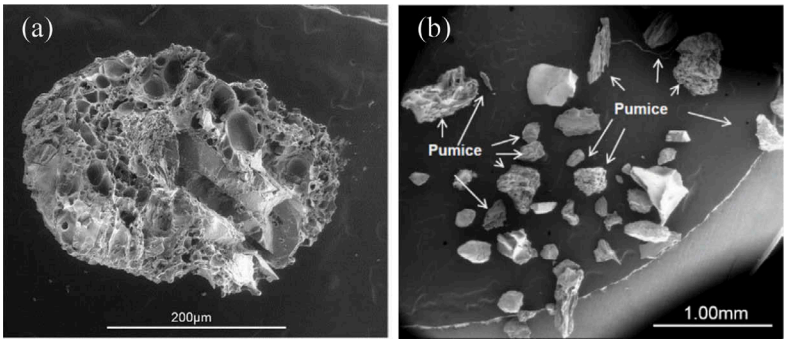

Figure 1. Scanning electron microscope (SEM) image of: (a) pumice particle; and (b) NP sands.

while some researches have been conducted on pure pumice sand and Japanese volcanic soils, there are very few information available for NP sands in terms of their liquefaction behavior (Asadi et al., 2019a; Orense et al., 2012).

To investigate the applicability of V_s-based approach in estimating the liquefaction resistance of NP sands, laboratory testing was employed due to better control of soil condition in terms of D_r and effective confining pressure (σ'_c). Cyclic triaxial tests and bender element tests were performed on reconstituted NP sands, and an attempt was made to find a correlation between V_s and *CRR* of these crushable soils. The results were then compared to that of Toyoura sand.

2 EXPERIMENTAL PROGRAMME

2.1 *Materials used*

The NP sands used for reconstituted testing were sourced from three sites in the Waikato basin in the central part of North Island (Figure 2). Bulk specimens of natural pumice 1 (NP1), natural pumice 2 (NP2) and natural pumice 3 (NP3) sands were obtained from road construction sites at target depths of 4.5 to 5 m, 5.95 to 6.85 m and 1.5 to 2 m, respectively. The index properties and particle size distribution (PSD) curves of the materials are shown in Table 1 and Figure 3, respectively. In addition, a series of laboratory tests was also performed on Toyoura sand, which is frequently used in laboratory studies and is known to be sub-angular and hard-grained. The Japanese standard method (JGS, 2000) was adopted to measure the maximum (ρ_{dmax}) and minimum (ρ_{dmin}) dry densities of the materials while the New Zealand standard NZS4402 (Standards New Zealand, 1986) was followed to determine the specific gravity (G_s). Note that the Japanese standard was used to eliminate particle crushing during maximum dry density test.

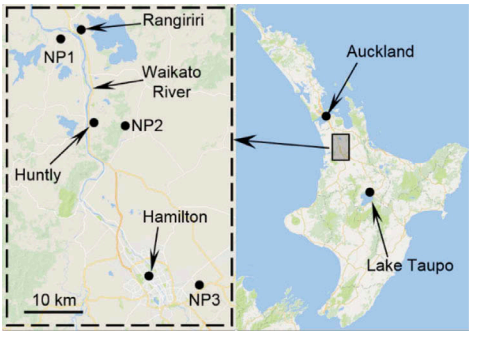

Figure 2. Sites where NP sands were collected from the central part of North Island.

Table 1. Index properties of tested materials.

Material	Specific gravity	Coefficient of uniformity	Maximum dry density (gr/cm^3)	Minimum dry density (gr/cm^3)
NP1 (Rangiriri)	2.54	4.90	1.24	0.93
NP2 (Huntly)	2.48	5.34	1.27	0.97
NP3 (Hamilton)	2.53	3.98	1.54	1.27
Toyoura sand	2.66	1.17	1.64	1.40

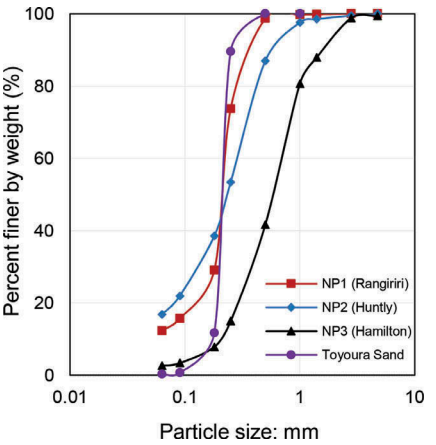

Figure 3. Particle size distribution curves of the tested materials.

2.2 *Sample preparation*

The reconstituted specimens were prepared by moist tamping method, with the target size of 63 mm diameter and 126 mm high. Before setting up the specimens, the soil materials were mixed with water (at approximately 20% water content) to form uniformly moist samples. Then, a pre-weighed quantity of the materials was poured in five layers into the split mold with a membrane held in place by external vacuum, with each layer compacted carefully to reach a specified initial relative density. Once a soil specimen reached the final target height, a special cap with the slot for the bender element was placed on the top of the specimen, with the slot oriented similarly to the bender element on the pedestal. Then, a groove was gently made on the specimen through the slot and the top cap was placed on top of the specimen to fit the bender element into the specimen, and the split mold was removed. Finally, the triaxial cell was assembled, the cell filled with water and the specimen was saturated by applying a back pressure of 600 kPa until a *B*-value greater than 0.96 was achieved.

2.3 *Bender element test*

Bender element test, a non-destructive dynamic test, was utilized to measure the shear wave velocity (V_s) of the specimens through the equation: $V_s = L/t$, where L is the tip-to-tip distance between the bender elements installed on top and bottom of the specimen, while t is the travel time of shear wave propagation through the specimen. Peak-to-peak arrival time method was chosen to measure t, owing to the consistency, clarity and simplicity of this method as compared to other approaches. The bender element system employed consisted of FG110 synthesized function generator and TDS 2024C digital oscilloscope for generating waves and recording the generated and received signals for post data analysis, respectively. The bender element test with pulse sinusoidal waves at frequencies of 3, 5, 7 and 9 kHz was

conducted on specimens of NP1, NP3 and Toyoura sands at various levels of post-consolidation void ratio (e) and a wide range of σ'_c=20 to 300 kPa, while that of NP2 was under σ'_c=20 to 100 kPa. The approach proposed by Verdugo & Ishihara (1996) was followed to measure the void ratio, e, at all levels of applied σ'_c.

2.4 *Undrained cyclic triaxial test*

A number of specimens were also isotropically consolidated under σ'_c=100 kPa, and then a servo hydraulic loading frame applied sinusoidal cyclic loading on the specimens with a frequency of 0.1 Hz under undrained condition. The specimens were subjected to different levels of cyclic stress ratio (CSR_{tx}) which is defined as $CSR_{tx} = q/2\sigma'_c$, where q is the deviator stress and measured as the difference between axial effective stress (σ'_1) and lateral effective stress (σ'_3), i.e. $q = \sigma'_1 - \sigma'_3$. During the cyclic triaxial test, once the double amplitude axial strain (ε_{DA}) reached 5%, the specimen was considered to have liquefied. Then, the liquefaction resistance curves of the specimens at various levels of e (corresponding to D_r=30, 50 and 80%) were developed by plotting CSR_{tx} against the number of cycles (N_c) required to liquefy the specimen. The liquefaction resistance ($CRR_{tx\text{-}15}$) was defined as the CSR_{tx} at which the specimen liquefied in N_c=15 cycles.

3 TEST RESULTS AND DISCUSSION

3.1 *Bender element test*

Figure 4a illustrates the developed best-fit lines of $V_s \sim e^{-m}$ relations of the tested sands under similar σ'_c=100 kPa, where m is the power coefficient of e. As evident from the figure, the V_s of NP1 and NP2 sands have a significantly lower dependency on e (i.e. m_{NP1}=0.31, m_{NP2}=0.20); however, NP3 and Toyoura sand show higher influence of e on the value of V_s (i.e. m_{NP3}=0.78, $m_{Toyoura}$=0.66). Furthermore, Figure 4b shows the $V_s \sim \sigma'^{n}_c$ relation (where n is power coefficient of σ'_c) of the materials with the best-fit lines under similar e (corresponding to D_r=55%) over the applied levels of σ'_c. The results presented indicate that the NP sands have higher $V_s \sim \sigma'_c$ dependency (i.e. n_{NP1}=0.36, n_{NP2}=0.37, n_{NP3}=0.30), when compared to Toyoura sand ($n_{Toyoura}$=0.25).

It can be seen from the figures that NP sands have generally lower V_s over a wide range of e and σ'_c when compared to Toyoura sand. Among NP sands, NP1 and NP2 have significantly lower V_s compared to NP3; as shown in Table 1, NP1 and NP2 have higher e_{max}, e_{min}, and void ratio range ($e_{max} - e_{min}$) and these lead to a certain e for a specified D_r. Thus, for the plots shown in the figures, NP1 and NP2 specimens have higher e and therefore have more voids than NP3 and Toyoura sand specimens. Furthermore, Figure 1a and X-ray CT scanning performed by Kikkawa et al. (2013) show that pumice particle is porous; the shear wave propagation in soft and porous soils would be lower than that in stiff and solid sand. Thus, it is expected that the V_s of NP1 and NP2 sands would be lower and less dependent on e (i.e. degree of packing) than that of NP3 and Toyoura sand. Moreover, the higher angularity

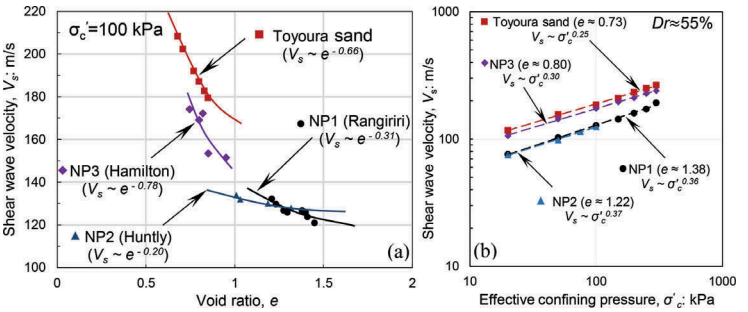

Figure 4. Relation of V_s to: (a) e; and (b) σ'_c of the tested materials.

and compressibility/crushability features of pumice particles make the NP sand assemblies to have better particle contacts at higher levels of σ'_c, which prevent segregation of particles leading to a continuum solid behavior, allowing for higher V_s at higher levels of σ'_c (i.e. higher n-value) when compared to Toyoura sand (Asadi et al., 2018a)

3.2 *Liquefaction resistance*

Figure 5 illustrates the liquefaction resistance curves of the materials over a wide range of relative densities (i.e. D_r=30, 50 and 80%) and under similar σ'_c=100 kPa. From the figures, the liquefaction resistance of NP sands is considerably higher than that of Toyoura sand. For instance, under similar D_r=80%, NP1, NP2 and NP3 have liquefaction resistance ($CRR_{tx\text{-}15}$) of 0.34, 0.29 and 0.46, respectively, while Toyoura sand has $CRR_{tx\text{-}15}$=0.24. Asadi et al. (2018b), who performed a number of undrained cyclic triaxial tests on NP sands as well as particle shape morphology and particle crushing investigations, reported that the higher $CRR_{tx\text{-}15}$ of NP sands may be attributed to the irregular surface texture and manifestation of pumice particle during cyclic loading, which helped in the formation of a more stable soil structure compared to Toyoura sand.

The plots of $CRR_{tx\text{-}15} \sim e^{-\beta}$ (where β is the power coefficient of e) of the tested specimens and the best-fit lines are illustrated in Figure 6. It can be seen that NP1 and NP2 have lower $CRR_{tx\text{-}15} \sim e$ dependency (i.e. β_{NP1}=2.17, β_{NP2}=1.75), while the effect of e is more pronounced on NP3 and Toyoura sand (i.e. β_{NP3}=3.38, $\beta_{Toyoura}$=3.82). The observed behavior in terms of $CRR_{tx\text{-}15} \sim e$ relation can be attributed again to the higher e as well as higher manifestation of particle crushing for NP1 and NP2 when compared to NP3 and Toyoura sands.

3.3 *$CRR_{Field} - V_{s1}$ chart for NP sands*

The laboratory results illustrated in Figure 4a (i.e. $V_s \sim e$) and Figure 6 (i.e. $CRR_{tx\text{-}15} \sim e$) were then utilized to develop the $CRR_{tx\text{-}15} \sim V_s$ correlations, following the laboratory-based

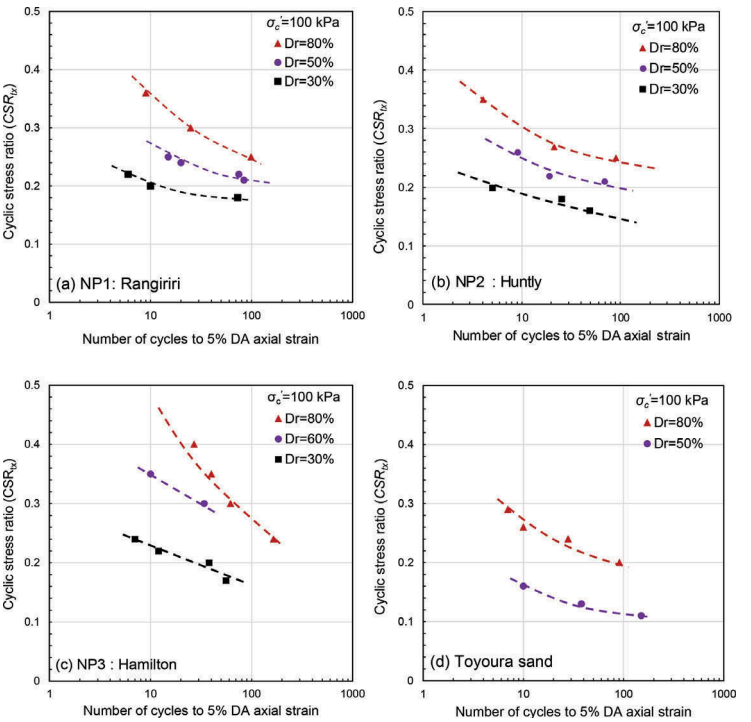

Figure 5. Liquefaction resistance curves of: (a) NP1; (b) NP2; (c) NP3 and (d) Toyoura sand.

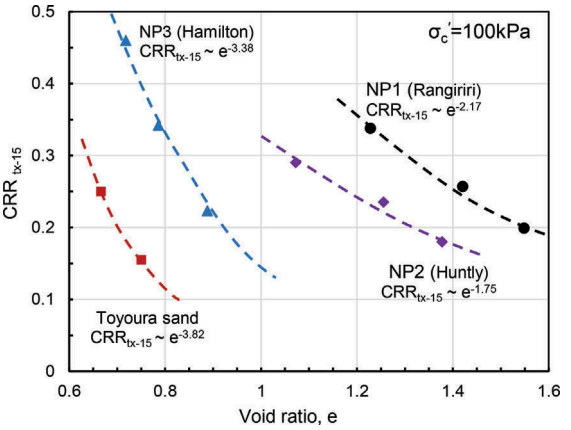

Figure 6. Effect of void ratio on the liquefaction resistance of tested materials.

approaches established by several researchers (e.g. Tokimatsu & Uchida, 1990; Zhou & Chen, 2007). To establish such correlations, initially the values of $CRR_{\text{tx-15}}$ and V_s obtained in the laboratory were converted into field condition (denoted as CRR_{Field} and V_{s1}, respectively), following empirical correlations available in the literature. Seed (1979) conversion method was followed to convert $CRR_{\text{tx-15}}$ into field condition as follows:

$$CRR_{\text{Field}} = \left(\frac{1+2K_0}{3}\right) r_c \; CRR_{\text{tx}-15} \tag{1}$$

where K_0 is coefficient of lateral earth pressure in field condition, while r_c is a constant value to consider the effect of multidirectional shaking in the field. Moreover, the values of V_s were converted into field condition using the following equation:

$$V_{s,\text{Field}} = V_s \left(\frac{1+2K_0}{3}\right)^n \tag{2}$$

where n is the power coefficient of σ'_c obtained from Figure 4b. Next, the $V_{s,\text{ Field}}$ was corrected for overburden pressure using the equation (Andrus & Stokoe, 2000):

$$V_{S1} = V_{S,\text{Field}} \left(\frac{P_a}{\sigma'_v}\right)^{0.25} \tag{3}$$

where σ'_v is the effective overburden pressure and P_a=100 kPa is the reference stress. Thus, the $CRR_{\text{Field}} - V_{s1}$ relations were established and plotted in Figure 7, where they are compared with those plots available for normal sands (e.g. Andrus & Stokoe, 2000; Zhou & Chen, 2007; Kayen at al., 2013). As seen in the figure, the curve for Toyoura sand plots in similar region as those for other normal sands. On the other hand, the plots for NP1 and NP2 are significantly far to the left of these curves, indicating that the $CRR_{\text{Field}} - V_{s1}$ curves for normal sands significantly underestimate the liquefaction resistance of these materials. Furthermore, the curve for NP3 is plotted between those of NP1 and NP2 and those for normal sands.

Comparing the 3 NP sands, the observed differences can also be attributed to the higher void ratios and possibly higher compressibility/crushability features of NP1 and NP2 specimens, which lead to their lower V_s when compared to NP3. The higher fines content (F_c) and higher coefficient of uniformity (C_u) for NP1 and NP2 may also have played a significant role on their low V_s, consistent with the observations of many researchers (e.g. Sahaphol & Miura., 2005; Cho et al., 2006). Finally, the amount of crushable pumice particles present,

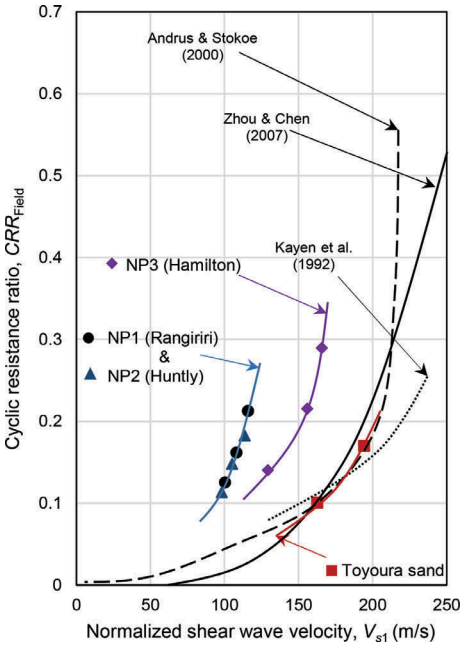

Figure 7. Comparison of $CRR_{Field} - V_{s1}$ charts developed for NP sands with those of hard-grained sands.

expressed in terms of pumice content (PC) may have important effect on the observed behavior. A study conducted by Asadi et al. (2019b) indicated that NP1 and NP2 sands have PC of ≈44% and ≈54%, respectively, while NP3 has PC≈18%. The lower PC of NP3 is a possible reason why its $CRR_{Field} - V_{s1}$ curve plots nearer to those of normal sands; further tests are planned to confirm this observation.

4 CONCLUSIONS

The applicability of V_s–based approach for liquefaction assessment of crushable natural pumiceous (NP) sands was investigated by performing bender element and cyclic triaxial tests on 3 different reconstituted NP sands (i.e. NP1, NP2 and NP3). For comparison, similar tests were also conducted on Toyoura sand. The following are the major conclusions from this study:

- NP sands showed lower V_s when compared to Toyoura sand under similar D_r and σ'_c, owing to the presence of crushable and porous pumice particles with irregular surface texture within their soil matrix. Comparing the 3 NP sands, they showed significant difference in terms of V_s, with NP1 and NP2 having considerably lower V_s compared to NP3; this can be explained through the different index properties and pumice contents of the NP sands.
- Under similar D_r and σ'_c, NP sands have significantly higher liquefaction resistance (CRR_{Field}) compared to Toyoura sand. Their higher CRR_{Field} may be due to the presence of angular pumice particles which provided better particles interlocking, accompanied by particle crushing, and resulted in more stable soil structure during application of cyclic loading.
- The $CRR_{Field} - V_{s1}$ curve for Toyoura sand plotted in similar zone as the normal sands available in the literature; however, NP1 and NP2 sands plotted far to the left side of the correlations for normal hard-grained sands. The plot for NP3 sand deviated from the other NP sands and was nearer to the normal sand plots, possibly due to lower pumice content.
- The observed behavior of NP sands indicated that the V_s - based approach developed for normal sands was not appropriate for estimating the liquefaction resistance of NP sands.

ACKNOWLEDGEMENTS

The authors would like to acknowledge the assistance of Tonkin + Taylor Ltd and Opus International Consultants Ltd in facilitating access to the site and in providing some samples and site details is gratefully acknowledged. The first author also gratefully acknowledges the PhD scholarship support from Natural Hazard Research Platform (NHRP).

REFERENCES

Andrus, R. D., & Stokoe, K. H. (2000). Liquefaction resistance of soils from shear-wave velocity. *Journal of Geotechnical and Geoenvironmental Engineering*, 126(11), 1015–1025.

Asadi, M. B., Asadi, M. S., Orense, R. P., & Pender, M. J. (2018a). Shear wave velocity-based assessment of liquefaction resistance of natrual pumiceous sands. *Geotechnique Letters*, 8 (4), 262–267.

Asadi, M. S., Asadi, M. B., Orense, R. P., & Pender, M. J. (2018b). Undrained cyclic behaviour of reconstituted natural pumiceous sands. *Journal of Geotechnical and Geoenviromental Engineering*, 144(8), 04018045.

Asadi, M. S., Orense, R. P., Asadi, M. B., & Pender, M. J. (2019a). Post-liquefaction behavior of natural pumiceous sands. *Soil Dynamic and Earthquake Engineering*, 118, 65–74.

Asadi, M. S., Orense, R. P., Asadi, M. B., & Pender, M. J. (2019b). Maximum dry density test to quantify pumice content in natural soils. *Soil and Foundation* [Accepted].

Cho, G. C., Dodds, J., & Santamarina, J. C. (2006). Particle shape effects on packing density, stiffness, and strength: Natural and crushed sands. *Journal of Geotechnical and Geoenvironmental Engineering*, 132(5), 591–602. 10.1061.

Japanese Geotechnical Society, JGS (2000). *Soil Test Procedure and Commentaries*, Revised 1st Ed., Tokyo (in Japanese).

Kayen, R., Moss, R.E.S., Thompson, E.M., Seed, R.B., Cetin, K.O., Kiureghian, A. D., Tanaka, Y., Tokimatsu, K. (2013). Shear wave velocity-based probabilistic and deterministic assessment of seismic soil liquefaction potential. *Journal of Geotechnical and Geoenvironmental Engineering*, 139(3), 407–419.

Kikkawa, N., Orense, R. P., & Pender, M. J. (2013). Observations on microstructure of pumice particles using computed tomography. *Canadian Geotechnical Journal*, *50*(11), 1109–1117.

Miura, S., Yagi, K., & Asonuma, T. (2003). Deformation-strength evaluation of crushable volcanic soils by laboratory and in-situ testing. *Soils and Foundations*, 43(4), 47–57.

Orense, R. P., Pender, M. J., & O'Sullivan, A. (2012). Liquefaction characteristics of pumice sands. *Report No. EQC 10l589*, University of Auckland, New Zealand.

Sahaphol, T., & Miura, S. (2005). Shear moduli of volcanic soils. *Soil Dynamics and Earthquake Engineering*, 25(2), 157–165.

Seed, H. B. (1979). Soil liquefaction and cyclic mobility evaluation for level ground during earthquakes. *Journal of the Geotechnical Engineering Division*, 105(2), 201–255.

Seed, H.B., & Idriss, I. M. (1971). Simplified procedure for evaluating soil liquefaction potential. *ASCE J Soil Mech Found Div, 97*(SM9), 1249–1273.

Seed, H. B., & Lee, K. L. (1966). Liquefaction of saturated sands during cyclic loading. *Journal of the Soil Mechanics and Foundation Division, 902 (6), 105–134*.

Standards New Zealand (1986). *NZS 4402: 1986 - Methods of Testing Soils for Civil Engineering Purposes*. Part 2 Soil classification tests. 2.7. Determination of the solid density of soil particles. Test 2.7.2 Method for medium and fine soils.

Tokimatsu, K., & Uchida, A. (1990). Correlation between liquefaction resistance and shear wave velocity. *Soils and Foundations*, *30*(2), 33–42.

Verdugo, R., & Ishihara, K. (1996). The steady state of sandy soils. *Soils and Foundations*, 36(2), 81–91.

Wesley, L. D. (2006). Geotechnical characteristics of a pumice sand. *Proc., 2nd International Workshop on Characterisation and Engineering Properties of Natural Soils*, 4, 2449–2473.

Youd, T.L., Idriss, I.M., Andrus, R.D., Arango, I., Castro, G., Christian, J.T., Dobry, R.,. . ..(2001). Liquefaction resistance of soils: Summary report from the 1996 NCEER and 1998 NCEER/NSF workshops on evaluation of liquefaction resistance of soils. *Journal of Geotechnical and Geoenvironmental Engineering*, 127(10), 817–833.

Zhou, Y. G., & Chen, Y. M. (2007). Laboratory investigation on assessing liquefaction resistance of sandy soils by shear wave velocity. *Journal of Geotechnical and Geoenvironmental Engineering*, 133(8), 959–972.